VOLUME 118, NUMBER 27
JULY 10, 1996

JOURNAL OF THE AMERICAN CHEMICAL SOCIETY

The Macrobicyclic Cryptate Effect in the Gas Phase

Qizhu Chen, Kevin Cannell, Jeremy Nicoll,† and David V. Dearden*,†

Contribution from the Department of Chemistry and Biochemistry, Box 19065, The University of Texas at Arlington, Arlington, Texas 76019-0065

Received October 16, 1995[⊗]

Abstract: The alkali cation (Li^+, Na^+, K^+, Rb^+, and Cs^+) binding properties of cryptands [2.1.1], [2.2.1], and [2.2.2] were investigated under solvent-free, gas-phase conditions using Fourier transform ion cyclotron resonance mass spectrometry. The alkali cations serve as size probes for the cryptand cavities. All three cryptands readily form 1:1 alkali cation complexes. Ligand−metal (2:1) complexes of [2.1.1] with K^+, Rb^+, and Cs^+, and of [2.2.1] with Rb^+ and Cs^+ were observed, but no 2:1 complexes of [2.2.2] were seen, consistent with formation of "inclusive" rather than "exclusive" complexes when the binding cavity of the ligand is large enough to accommodate the metal cation. Kinetics for 2:1 ligand−metal complexation, as well as molecular mechanics calculations and cation transfer equilibrium constant measurements, lead to estimates of the radii of the cation binding cavities of the cryptands under gas-phase conditions: [2.1.1], 1.25 Å; [2.2.1], 1.50 Å; [2.2.2], 1.65 Å. Cation transfer equilibrium studies comparing cryptands with crown ethers having the same number of donor atoms reveal that the cryptands have higher affinities than crowns for cations small enough to enter the cavity of the cryptand, while the crowns have the higher affinity for cations too large to enter the cryptand cavity. The results are interpreted in terms of the macrobicyclic cryptate effect: for cations small enough to fit inside the cryptand, the three-dimensional preorganization of the ligand leads to stronger binding than is possible for a floppier, pseudo-two-dimensional crown ether. The loss of binding by one ether oxygen which occurs as metal size increases for a given cryptand is worth approximately 25 kJ mol^{-1}, and accounts for the higher cation affinities of the crowns for the larger metals. The Li^+ affinity of 1,10-diaza-18-crown-6 is ∼1 kJ mol^{-1} higher than that of 18-crown-6, while the latter has lower affinity than the former for all of the larger alkali cations (about 7 kJ mol^{-1} lower for Na^+, and about 15 kJ mol^{-1} lower for K^+, Rb^+, and Cs^+). The equilibrium measurements also allow the determination of relative free energies of cation binding for a number of crown ethers and cryptands. Molecular mechanics modeling with the AMBER force field is generally consistent with the experiments.

Introduction

Cryptands are relatively rigid, macrobicyclic ligands structurally related to crown ethers (Figure 1), named using numbers to specify the number of ethoxide units in each of the three bridges between the bridgehead nitrogens. Since the initial report of their synthesis by Lehn and co-workers,[1,2] the cryptands and their complexes ("cryptates") have been extensively investigated.[3−8] Cryptands share with crowns the remarkable ability to selectively bind metal cations: in 95:5 methanol−

† Present Address: Department of Chemistry and Biochemistry, C100 Benson Science Building, Brigham Young University, Provo, Utah 84602-5700.

⊗ Abstract published in *Advance ACS Abstracts,* June 15, 1996.

(1) Dietrich, B.; Lehn, J. M.; Sauvage, J. P.; Blanzat, J. *Tetrahedron* **1969**, *29*, 1629.
(2) Dietrich, B.; Lehn, J. M.; Sauvage, J. P. *Tetrahedron Lett.* **1969**, 2885.
(3) Lehn, J.-M. *Acc. Chem. Res.* **1978**, *11*, 49−57.
(4) Dietrich, B. In *Inclusion Compounds*; Atwood, J. L., Davies, J. E. D., MacNicol, D. D., Eds.; Academic: London, 1984; Vol. 2, pp 337−405.
(5) Buschmann, H. J. In *Stereochemical and Stereotypical Behavior of Macrocycles*; Bernal, I., Ed.; Elsevier: New York, 1987; pp 103−185.

S0002-7863(95)03460-3 CCC: $12.00

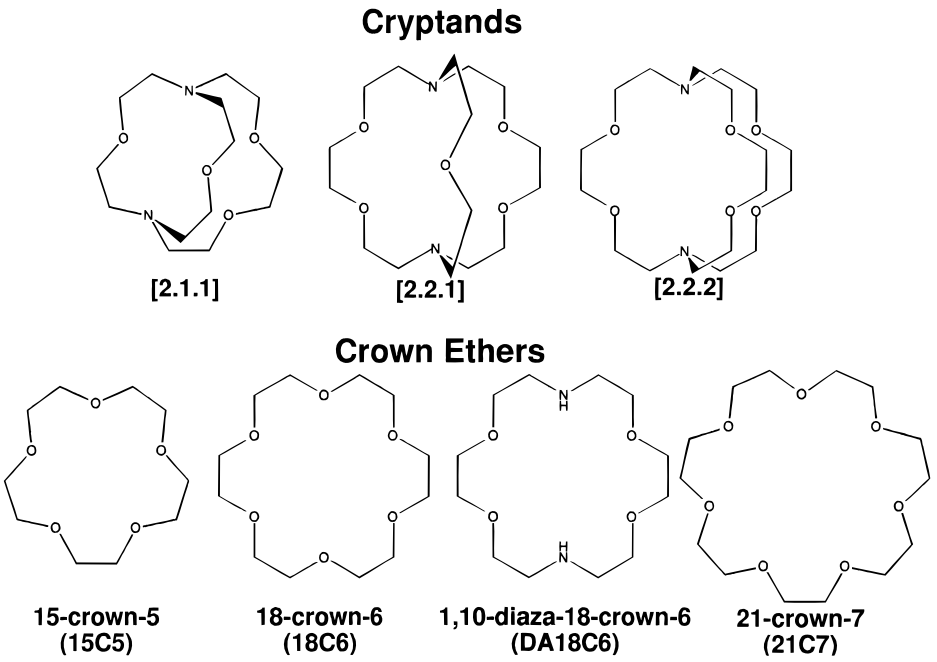

Figure 1. Structures and abbreviations for cryptands and crown ethers.

water solution, [2.1.1] selectively binds Li^+, [2.2.1] is selective for Na^+, and [2.2.2] is selective for K^+ over the other alkali metal ions.[3,9] In fact, these cryptands surpass the crown ethers in both complexation selectivity and complex stability for the selected ions.[7,8] A quick comparison of the architectures of crown ethers and cryptands reveals that while the oxygen donor atoms of the crowns are all in one ring, and therefore are confined by the ligand backbone to a pseudo-plane, in the bicyclic cryptands the oxygen and nitrogen donors are prearranged three-dimensionally, in a geometry better suited for binding spherically symmetric cations like the alkali metal ions.[9] The resulting increase in complex stability and selectivity has been termed the "macrobicyclic cryptate effect".[9]

Prior investigations of cryptands and their complexes include X-ray crystallographic structure determinations,[10] measurements of complexation stability constants in a number of solvent systems using a wide range of methods,[7,8] and NMR studies.[11−17] Cryptands and cryptates have also frequently been investigated by molecular modelers using various force fields and molecular dynamics methods.[18−22] In the gas phase, perfluorinated cryptands have been observed to bind anions,[23,24] and the affinity of [2.2.2] for alkali metal cations has been found to be less than that of the naturally-occurring ionophore valinomycin.[25,26]

Our interest in cryptands stems from our ongoing investigation of molecular recognition in gas-phase ion−molecule chemistry. Most prior work in this field has involved crown ethers,[23,27−42] which exhibit size-selective reactivity[43,44] and

(6) Christensen, J. J.; Eatough, D. J.; Izatt, R. M. *Chem. Rev.* **1974**, *74*, 351−384.
(7) Izatt, R. M.; Bradshaw, J. S.; Nielsen, S. A.; Lamb, J. D.; Christensen, J. J.; Sen, D. *Chem. Rev.* **1985**, *85*, 271−339.
(8) Izatt, R. M.; Pawlak, K.; Bradshaw, J. S.; Bruening, R. L. *Chem. Rev.* **1991**, *91*, 1721−2085.
(9) Lehn, J.-M.; Sauvage, J.-P. *J. Am. Chem. Soc.* **1975**, *97*, 6700−6707.
(10) Dobler, M. *Ionophores and Their Structures*; Wiley: New York, 1981.
(11) Lehn, J. M.; Sauvage, J.-P.Dietrich, B. *J. Am. Chem. Soc.* **1970**, *92*, 2916−2918.
(12) Ceraso, J. M.; Dye, J. L. *J. Am. Chem. Soc.* **1973**, *95*, 4432−4434.
(13) Kintzinger, J. P.; Lehn, J. M. *J. Am. Chem. Soc.* **1974**, *96*, 3313−3314.
(14) Cahen, Y. M.; Dye, J. L.; Popov, A. I. *J. Phys. Chem.* **1975**, *79*, 1289.
(15) Mei, E.; Liu, L.; Dye, J. L.; Popov, A. I. *J. Solution Chem.* **1977**, *6*, 771−778.
(16) Mei, E.; Popov, A. I.; Dye, J. L. *J. Am. Chem. Soc.* **1977**, *99*, 6532−6536.
(17) Kauffman, E.; Dye, J. L.; Lehn, J.-M.; Popov, A. I. *J. Am. Chem. Soc.* **1980**, *102*, 2274−2278.
(18) Wipff, G.; Kollman, P. *New J. Chem.* **1985**, *9*, 457−465.
(19) Auffinger, P.; Wipff, G. *J. Comput. Chem.* **1990**, *11*, 19−31.
(20) Auffinger, P.; Wipff, G. *J. Chim. Phys. Phys.-Chim. Biol.* **1991**, *88*, 2525−2534.
(21) Auffinger, P.; Wipff, G. *J. Am. Chem. Soc.* **1991**, *113*, 5976−5988.
(22) Wipff, G. *J. Coord. Chem.* **1992**, *27*, 7−37.
(23) Brodbelt, J.; Maleknia, S.; Lagow, R.; Lin, T. Y. *J. Chem. Soc., Chem. Commun.* **1991**, 1705−1707.
(24) Lin, T.-Y.; Lin, W.-H.; Clark, W. D.; Lagow, R. J.; Larson, S. B.; Simonsen, S. H.; Lynch, V. M.; Brodbelt, J. S.; Maleknia, S. D.; Liou, C.-C. *J. Am. Chem. Soc.* **1994**, *116*, 5172−5179.
(25) Wong, P. S. H.; Antonio, B. J.; Dearden, D. V. *J. Am. Soc. Mass Spectrom.* **1994**, *5*, 632−637.
(26) Wilson, S. R.; Wu, Y. *Supramol. Chem.* **1994**, *3*, 273−277.
(27) Meot-Ner, M. *J. Am. Chem. Soc.* **1983**, *105*, 4906−4911.
(28) Meot-Ner, M. *J. Am. Chem. Soc.* **1983**, *105*, 4912−4915.
(29) Sharma, R. B.; Blades, A. T.; Kebarle, P. *J. Am. Chem. Soc.* **1984**, *106*, 510−516.
(30) Sharma, R. B.; Kebarle, P. *J. Am. Chem. Soc.* **1984**, *106*, 3913−3916.
(31) Katritzky, A. R.; Malhotra, N.; Ramanathan, R.; Kemerait, R. C.; Zimmerman, J. A.; Eyler, J. R. *Rapid Commun. Mass Spectrom.* **1992**, *6*, 25−27.
(32) Brodbelt, J.; Maleknia, S.; Liou, C. C.; Lagow, R. *J. Am. Chem. Soc.* **1991**, *113*, 5913−5914.
(33) Maleknia, S.; Brodbelt, J. *J. Am. Chem. Soc.* **1992**, *114*, 4295−4298.
(34) Maleknia, S.; Brodbelt, J. *Rapid Commun. Mass Spectrom.* **1992**, *6*, 376−381.
(35) Liou, C. C.; Brodbelt, J. S. *J. Am. Soc. Mass Spectrom.* **1992**, *3*, 543−548.
(36) Liou, C. C.; Brodbelt, J. S. *J. Am. Chem. Soc.* **1992**, *114*, 6761−6764.
(37) Liou, C. C.; Brodbelt, J. S. *J. Am. Soc. Mass Spectrom.* **1993**, *4*, 242−248.
(38) Wu, H.-F.; Brodbelt, J. S. *J. Am. Soc. Mass Spectrom.* **1993**, *4*, 718−722.
(39) Brodbelt, J. S.; Liou, C.-C.; Maleknia, S.; Lin, T.-Y.; Lagow, R. J. *J. Am. Chem. Soc.* **1993**, *115*, 11069−11073.
(40) Wu, H.-F.; Brodbelt, J. S. *J. Am. Chem. Soc.* **1994**, *116*, 6418−6426.
(41) Medina, J. C.; Goodnow, T. T.; Rojas, M. T.; Atwood, J. L.; Lynn, B. C.; Kaifer, A. E.; Gokel, G. W. *J. Am. Chem. Soc.* **1992**, *114*, 10583−10595.

pronounced macrocyclic effects[34,44,45] in the gas phase. The present investigation of cryptands and their alkali metal complexes extends the gas-phase studies from the pseudo-two-dimensional crowns to three-dimensional ligands, and allows a number of important new questions to be addressed. For example, in this paper we show that cryptands exhibit remarkable size selectivity even in the absence of solvent, and discuss how solvation affects the recognition capabilities of these ligands. Further, the relative cation affinities of crown ethers and cryptands are compared, and the macrobicyclic cryptate effect is observed and characterized for the first time in the gas phase.

Experimental Section

FTICR/MS Experiments. The experimental apparatus and procedures used in these experiments have been described.[44] In brief, alkali metal cations were produced by excimer-pumped dye laser (Lambda-Physik) desorption of the appropriate alkali metal salts in the high magnetic field region of a Fourier transform ion cyclotron resonance mass spectrometer (FTMS 1000, Extrel FTMS, Waters Corp., Madison, WI). The trapping cell was a custom-built, capacitively-coupled open cell based on the design of Beu and Laude.[46,47] Trapping potentials of 1 V were typically used. The excitation RF amplifier of this instrument was modified by adding a second stage of amplification, boosting the maximum excitation amplitude to approximately 200 V_{pp}. This modification greatly facilitated both ion isolation and detection. For equilibrium experiments, typically two neutral ligands were introduced through vacuum locks into the vacuum chamber on two independent, thermally-regulated direct exposure solid sample probes. A few experiments were repeated using electrospray ionization to generate alkali metal cryptates in an external-source Fourier transform ion cyclotron resonance instrument (APEX 47e, Bruker Instruments, Billerica, MA), with results in agreement with those obtained using laser desorption. All of the ligands were obtained from Aldrich (Milwaukee, WI) except 21C7, which was purchased from Parish Chemical Co. (Orem, UT). All were used without further purification.

Vapor pressures sufficient for our experiments were attained at ambient temperature for all the ligands studied. The total pressure in the vacuum chamber was typically in the range 5×10^{-8} to 5×10^{-7} Torr, as indicated by a Bayard-Alpert ionization gauge mounted external to the magnetic field (actual pressures in the trapping cell were probably higher). The *relative* pressures of the two ligands were determined by measuring the rates of proton attachment (from an acid such as a protonated crown fragment ion or protonated acetone) to each of the ligands.[44,48,49] This was accomplished by using the normalized signal intensity of the protonated molecular ion of one of the ligands as a function of time as the *x*-coordinate and of the other ligand as the *y*-coordinate. A plot of such data yields a straight line. If it is assumed that the efficiency of proton transfer to each of the two ligands is similar, the slope of this plot gives the pressure ratio of the two ligands being compared. This assumption is probably a good one, because it is well-known that the efficiencies of exothermic proton transfers are usually 90% or greater,[50] and all of the reactions employed are clearly exothermic. Further, while the crown ethers and cryptands being compared are not homologs, they are all cyclic polyethers, structurally similar enough that we expect the proton trnasfer efficiencies to be similar, so errors in the pressure ratios should be small.

The use of FTICR/MS techniques to measure equilibrium constants has been discussed in detail.[51] Typically, ion−molecule complexes were allowed to form in the trapping cell, after which complexes of one of the ligands with several (usually 3 or more) alkali cations were isolated using standard swept-RF techniques. The isolated complexes were then allowed to react with the neutral ligands in the chamber until equilibrium was attained. Reaction times ranging from about 1 s to about 60 s were required, depending on the ligands involved and on pressure conditions. Two criteria verified the attainment of equilibrium. First, the ratios of the signals from the ion−molecule complex species involving the two ligands being compared were observed to become constant. Second, equilibrium was approached using complexes with each of the ligands as the initial reactants, and the same equilibrium constants were obtained regardless of the direction of approach. These procedures ensure that the various metals experience identical ligand pressure conditions, so that the relative values of the equilibrium constants as the metal is varied for a given set of ligands are highly accurate. The reported results are means of three or more determinations, with standard deviations listed.

Thermochemical data were derived from the equilibrium constant measurements by assuming thermal equilibrium at a temperature of 350 K in the trapping cell. Temperatures were measured using a thermocouple mounted in the solid sample probe from which the ligands were evaporated into the vacuum chamber. Heating of the cell above ambient temperatures was due to the electron ionization filament, which was left on during all experiments (although electrons were pulsed through the cell only during pressure measurements). Use of the filament means that there was a temperature gradient across the trapping region. A temperature of 350 K represents a typical value obtained at the solids probe with the instrument in operation, and the fact that all experiments were conducted within 10 K of this value ensures that the data are internally consistent.

The largest likely source of error in the thermochemical results arises from potential errors in the pressure measurements for the two neutrals. However, even if the pressure ratios are wrong by as much as a factor of 4, this introduces an error of only about 4 kJ mol^{-1} in the free energy results. Finally, we note that since the experiments compared the various metals under identical ligand pressure and temperature conditions, the trends as the metals are varied for a given pair of ligands should be highly accurate. The accuracy of the relative values as the metals are varied is probably limited by the reproducibility of the equilibrium constants.

Molecular Modeling. Model calculations were performed with version 3.0 of the HyperChem package (Autodesk Inc., Sausalito, CA) running on a 486DX2-66MHz microprocessor. All the structures were obtained using the AMBER force field distributed with HyperChem, modified by addition of nonbonded interaction parameters, taken from the literature,[18,52] for the alkali metal cations. Partial charges on the atoms of the neutral ligands were determined using single-point AM1 calculations. Polarization of the ligands by Li^+, Na^+, and K^+ was approximated using an iterative mixed-mode procedure wherein charges were calculated for the free ligand using AM1, the metal was added, the structure was minimized with AMBER, then the AM1 single-point calculation was repeated for the ligand in the presence of the metal. The AMBER-AM1 cycle was repeated until no further change in partial charges was observed. Since the program does not support mixed-mode calculations for alkali cations larger than K^+, the partial charges in the K^+ cryptates were used for the ligands in AMBER calculations involving Rb^+ and Cs^+.

Molecular dynamics calculations were used to aid in conformational searching. In the simulations, the complexes were heated to 400 K and potential energy was plotted as a function of simulation time. Conformations at local potential energy minima were used as starting points for full AMBER geometry optimization. While this procedure cannot guarantee location of global minima, it did tend to reproducibly locate low-lying conformations. The structures reported are the lowest energy structures found.

(42) Takahashi, T.; Uchiyama, A.; Yamada, K.; Lynn, B. C.; Gokel, G. W. *Tetrahedron Lett*. **1992**, *33*, 3825−3828.
(43) Zhang, H.; Chu, I.-H.; Leming, S.; Dearden, D. V. *J. Am. Chem. Soc*. **1991**, *113*, 7415−7417.
(44) Chu, I. H.; Zhang, H.; Dearden, D. V. *J. Am. Chem. Soc*. **1993**, *115*, 5736−5744.
(45) Zhang, H.; Dearden, D. V. *J. Am. Chem. Soc*. **1992**, *114*, 2754−2755.
(46) Beu, S. C.; Laude, D. A. *Anal. Chem*. **1992**, *64*, 177−180.
(47) Beu, S. C.; Laude, D. A. *Int. J. Mass Spectrom. Ion Proc*. **1992**, *112*, 215−230.
(48) Meot-Ner, M. *J. Phys. Chem*. **1980**, *84*, 2716−2723.
(49) Chu, I.-H.; Dearden, D. V.; Bradshaw, J. S.; Huszthy, P.; Izatt, R. M. *J. Am. Chem. Soc*. **1993**, *115*, 4318−4320.
(50) Su, T.; Bowers, M. T. In *Gas Phase Ion Chemistry*; Bowers, M. T., Ed.; Academic: New York, 1979; Vol. 1, pp 83−118.
(51) Operti, L.; Tews, E. C.; Freiser, B. S. *J. Am. Chem. Soc*. **1988**, *110*, 3847−3853.
(52) Kollman, P. A.; Wipff, G.; Singh, U. C. *J. Am. Chem. Soc*. **1985**, *107*, 2212−2219.

Table 1. Stoichiometry of Cryptand−Alkali Metal Complexes Observed in the Gas Phase

		cations with ionic radii (Å)[a]				
cryptand	cavity radius (Å)[b]	Li^+ 0.60	Na^+ 0.95	K^+ 1.33	Rb^+ 1.48	Cs^+ 1.69
[2.1.1]	0.8	1:1	1:1	1:1, 2:1	1:1, 2:1	1:1, 2:1
[2.2.1]	1.1	1:1	1:1	1:1	1:1, 2:1	1:1, 2:1
[2.2.2]	1.4	1:1	1:1	1:1	1:1	1:1

[a] Reference 55. [b] Reference 9.

Results

Observed Complexes. Metal−ligand 1:1 complexes were observed for all combinations of alkali metal cation with the ligands [2.1.1], [2.2.1], and [2.2.2]. Observed ligand−metal 2:1 complexes are listed in Table 1. At reaction delays of more than a few hundred milliseconds at the pressures employed, the 1:1 and 2:1 complexes completely dominate the mass spectra.

Equilibrium Constants. Equilibrium, as defined by the criteria above, was observed for many reactions involving transfer of a metal cation between two ligands. Equilibrium constants, measured at ambient temperature (350 K), are listed in Table 2.

Transfers of Li^+, Na^+, and K^+ from 15C5 to [2.1.1] were all observed to be exothermic, with the magnitude of the equilibrium constant decreasing with increasing cation size. The larger alkali cations were not examined with these ligands because the interfering formation of $(15C5)_2M^+$ is rapid.

Li^+ and Na^+ were observed to transfer exothermically from 18C6 to [2.1.1]. The analogous reactions for K^+, Rb^+, and Cs^+ were endothermic. Transfers of all the alkali cations examined from 18C6 to either [2.2.1] or [2.2.2] were exothermic. In none of these cases was formation of the 2:1 ligand−metal complexes so rapid as to interfere with the equilibrium determinations.

Transfers from 21C7 to cryptands were also examined. Li^+, Na^+, and K^+ were observed to transfer exothermically to [2.2.1], while the same reactions for Rb^+ and Cs^+ were endothermic. Transfer of all the alkali metal cations except Cs^+ from 21C7 to [2.2.2] was exothermic; Cs^+ transfer was slightly endothermic.

Metal exchange between cryptands was studied in a few cases. For transfer from [2.1.1] to [2.2.1], reactions involving all the alkali cations except Li^+ were exothermic, while Li^+ was preferentially bound by the smaller ligand. Transfer of Li^+ from [2.1.1] to [2.2.2], however, was found to be exothermic. Using the two larger cryptands, K^+, Rb^+, and Cs^+ transfers were exothermic from [2.2.1] to [2.2.2], while exchange of Na^+ was within experimental error of thermoneutral.

Molecular Models. Low-energy conformations found for the alkali metal cryptates of [2.1.1] are shown in Figure 2a. Molecular mechanics calculations with the AMBER force field predict that Li^+ is bound inside the cavity of [2.1.1], while Na^+ is bound somewhat above the center of mass of the ligand, but approximately in the center of the largest face, a 15-membered ring. The results for complexes of the larger alkali cations are very similar to those for the Na^+ complex, but place the metal above the 15-membered face, with the distance above the face increasing as cation radius increases.

Models of the [2.2.1] cryptates are shown in Figure 2b. The ligand adopts a somewhat distorted conformation in wrapping around Li^+, while the Na^+ complex exhibits a higher degree of symmetry. The Na^+ cation lies slightly off the N−N axis, but is still well within the cavity of the ligand. In the K^+ complex, the metal is positioned slightly above the 18-membered face of the ligand, being cupped in that face. The 18-membered face opens up to accommodate the larger Rb^+ and Cs^+ cations, which lie well above the binding cavity.

The lowest-energy structures found for the [2.2.2] cryptates are shown in Figure 2c. All of the alkali metal cations except Cs^+ are located inside the binding cavity of the ligand. In the K^+ and Rb^+ cryptates, the metal lies approximately at the center of mass of the ligand, while in the Li^+ and Na^+ cryptates it is off-center. In the Cs^+ cryptate, the metal lies outside the binding cavity, above one of the 18-membered faces of the ligand.

Discussion

Cavity Sizes for Gas-Phase Cryptands. While mass spectrometry is an excellent method for determining molecular structure in terms of atom connectivities, it is extremely difficult to experimentally determine the three-dimensional structure, or molecular shape, for gas-phase species, especially ions. Our experiments attempt to address this problem through using ion−molecule reactions as size probes. In particular, alkali metal cations are useful in this regard since they are inert with respect to bond insertion reactions, they have no low-lying excited states which might complicate their reactivity, and they span a range of sizes useful for probing small molecular ligands. In the subsequent discussion, we adopt a simple definition for ligand cavity size in the gas phase, based on the size of the largest cation which "fits" within the cavity.

Earlier studies of the complexation of alkali metal cations by the simple crown ethers 12C4, 15C5, 18C6, and 21C7 in the gas phase,[43,44] as well as by isomers of the alkyl-substituted crown dicyclohexano-18-crown-6,[53] found a strong correlation between the rate of formation of 2:1 ligand−metal complexes and the ratio of ligand cavity radius to guest ionic radius. In cases where the cations were small enough to enter the ligand binding cavity, 2:1 complex formation was too slow to observe, but for cations too large to enter the ligand cavity, 2:1 complexation occurred readily. It was postulated that cations small enough to enter the cavity are effectively encapsulated in the 1:1 complexes, preventing close enough approach by a second ligand to allow easy attachment.

The same simple model elegantly explains the results for the cryptands. The approximate radius of the [2.1.1] cavity has been estimated from CPK models to be about 0.8 Å.[9] In solid crystals, X-ray data indicate Li^+ binds within the cavity of [2.1.1], with all six heteroatoms coordinating the metal at distances close to the sum of the van der Waals radii.[54] In the gas phase, 1:1 complexes of Li^+ and Na^+ with [2.1.1] were observed, while 2:1 complexes were not seen. With all the larger alkali cations, both 1:1 and 2:1 complexes were seen. By analogy with the crown ether results, the [2.1.1] binding cavity must be large enough under gas-phase conditions to accommodate Na^+ (ionic radius 0.95 Å),[55] at least to the extent that close approach of a second ligand is not facile. On the other hand, [2.1.1] is too small for K^+ (ionic radius 1.33 Å).[55]

From CPK models, the cavity radius of [2.2.1] was estimated to be about 1.1 Å.[9] In X-ray studies of complexes of Na^+ and K^+ thiocyanates with [2.2.1],[56] Na^+ was found to be centrally located in the binding cavity. In the K^+ complex, the cation was not in the central cavity, but was observed centered in the 18-membered ring formed by the largest portal of the ligand,

(53) Chu, I.-H.; Dearden, D. V. *J. Am. Chem. Soc*. **1995**, *117*, 8197−8203.
(54) Moras, P. D.; Weiss, R. *Acta Crystallogr. Sect. B* **1973**, *29*, 400−403.
(55) Shannon, R. D. *Acta Crystallogr., Sect. A: Found. Crystallogr*. **1976**, *32*, 751−767.
(56) Mathieu, F.; Metz, B.; Moras, D.; Weiss, R. *J. Am. Chem. Soc*. **1978**, *100*, 4412−4416.

Table 2. log K and $\Delta G°$ (T = 350 K) for Cation Transfer between Gas Phase Ligands

reaction	cation	log K	$\Delta G°$, kJ mol^{-1}
$15C5M^+ + [2.1.1] \rightleftharpoons 15C5 + [2.1.1]M^+$	Li^+	2.65 ± 0.14	−17.76 ± 0.94
	Na^+	1.58 ± 0.18	−10.59 ± 1.21
	K^+	0.42 ± 0.11	−2.81 ± 0.74
$18C6M^+ + [2.1.1] \rightleftharpoons 18C6 + [2.1.1]M^+$	Li^+	2.29 ± 0.19	−15.34 ± 1.27
	Na^+	1.83 ± 0.13	−12.26 ± 0.87
	K^+	−0.91 ± 0.13	6.10 ± 0.87
	Rb^+	−1.56 ± 0.10	10.45 ± 0.67
	Cs^+	−1.16 ± 0.22	7.77 ± 1.47
$18C6M^+ + [2.2.1] \rightleftharpoons 18C6 + [2.2.1]M^+$	Li^+	1.87 ± 0.11	−12.53 ± 0.74
	Na^+	1.53 ± 0.08	−10.25 ± 0.54
	K^+	1.36 ± 0.15	−9.11 ± 1.01
	Rb^+	1.50 ± 0.06	−10.05 ± 0.40
	Cs^+	1.50 ± 0.06	−10.05 ± 0.40
$18C6M^+ + [2.2.2] \rightleftharpoons 18C6 + [2.2.2]M^+$	Li^+	2.61 ± 0.20	−17.49 ± 1.34
	Na^+	1.30 ± 0.12	−8.71 ± 0.80
	K^+	1.60 ± 0.03	−10.72 ± 0.20
	Rb^+	2.08 ± 0.33	−13.94 ± 2.21
	Cs^+	2.27 ± 0.25	−15.21 ± 1.68
$21C7M^+ + [2.2.1] \rightleftharpoons 21C7 + [2.2.1]M^+$	Li^+	1.52 ± 0.13	−10.18 ± 0.87
	Na^+	1.43 ± 0.11	−9.58 ± 0.74
	K^+	1.28 ± 0.21	−8.58 ± 1.41
	Rb^+	−0.30 ± 0.08	2.01 ± 0.54
	Cs^+	−2.17 ± 0.14	14.54 ± 0.94
$21C7M^+ + [2.2.2] \rightleftharpoons 21C7 + [2.2.2]M^+$	Li^+	1.24 ± 0.26	−8.31 ± 1.74
	Na^+	1.47 ± 0.23	−9.85 ± 1.54
	K^+	1.93 ± 0.12	−12.93 ± 0.80
	Rb^+	1.77 ± 0.12	−11.86 ± 0.80
	Cs^+	−0.15 ± 0.07	1.01 ± 0.47
$[2.1.1]M^+ + [2.2.1] \rightleftharpoons [2.1.1] + [2.2.1]M^+$	Li^+	−0.18 ± 0.08	1.21 ± 0.54
	Na^+	1.63 ± 0.09	−10.92 ± 0.60
	K^+	2.51 ± 0.07	−16.82 ± 0.47
	Rb^+	1.43 ± 0.10	−9.58 ± 0.67
	Cs^+	1.23 ± 0.03	−8.24 ± 0.20
$[2.1.1]M^+ + [2.2.2] \rightleftharpoons [2.1.1] + [2.2.2]M^+$	Li^+	0.23 ± 0.12	−1.54 ± 0.80
$[2.2.1]M^+ + [2.2.2] \rightleftharpoons [2.2.1] + [2.2.2]M^+$	Na^+	−0.02 ± 0.03	0.13 ± 0.20
	K^+	1.67 ± 0.20	−11.19 ± 1.34
	Rb^+	1.71 ± 0.13	−11.46 ± 0.87
	Cs^+	1.94 ± 0.05	−13.00 ± 0.34

and one of the eight coordination sites was occupied by the thiocyanate anion. Li^+, Na^+, and K^+ form 1:1 complexes with [2.2.1] in the gas phase, but 2:1 complexes were not seen. With the larger Rb^+ and Cs^+, 2:1 complexes were observed, suggesting that the [2.2.1] cavity in the gas phase can accommodate K^+ (ionic radius 1.33 Å), but not the slightly larger Rb^+ (ionic radius 1.48 Å).

There is evidence for "inclusive" structures for all the alkali cation complexes with [2.2.2] in condensed media. X-ray structures determined for Na^+, K^+, Rb^+, and Cs^+−[2.2.2] cryptates all have the metal in the central binding cavity of the ligand.[10] For the larger ions, this is somewhat surprising since CPK models suggest a cavity radius of only 1.4 Å for [2.2.2],[9] and each face of the ligand is an 18-membered ring similar to 18C6, which is much too small to accommodate Cs^+ (ionic radius 1.69 Å). In fact, in solution there is evidence for both internally and externally bound Cs^+. NMR experiments with $[2.2.2]Cs^+$ cryptates in methanol, nitropropane, and tetrahydrofuran solutions found that the cation shifts from an inside binding site at low temperatures to an outside site at higher temperature.[17] Ion pairing was believed to hinder formation of the "inclusive" Cs^+ complexes. However, in these complexes in the solid state, the C−C torsion angles increase to enlarge the cavity sufficiently to allow entry of the larger cations.[10] In the gas phase, the solvation and ion-pairing forces which might favor "exclusive" structures are absent, so "inclusive" geometries are probably more likely in a solvent-free environment. We note that all the alkali metal cations readily formed 1:1 cryptates of [2.2.2] in the gas phase, but no 2:1 complexes were observed, implying that all the alkali cations, including the large Cs^+ cation, are bound far enough inside the cryptand that approach of a second ligand and formation of a 2:1 complex is not facile.

For all three cryptands, the complexation results suggest slightly larger cavities than are predicted from CPK models or observed in the solid state (except in the case of $[2.2.2]Cs^+$ crystals). It is possible that 2:1 complexation in the gas phase is hindered when the metals can fit into one of the faces of the ligand; i.e. that complete entry into the central cavity is not necessary to slow addition of the second ligand to the extent that it is not observed. The binding of K^+ by 18C6, for example, is a case where the cation is nearly a perfect fit for the ligand cavity, according to X-ray results,[10] and in the gas phase, the $(18C6)K^+$ complex adds a second 18C6 ligand only very slowly.[44] Due to the more puckered ring conformation expected for the cryptands, these effects might be even more pronounced at a given ring cavity/cation radius ratio than for the crowns. In that case, alkali cation probes would tend to overestimate the cryptand cavity size. Examination of space-filling versions of the AMBER models supports this interpretation, except in the case of $[2.2.2]Cs^+$. For that model, the Cs^+ lies well outside the binding cavity of the ligand. However, it is possible this model structure does not represent the global minimum geometry. Similar calculations by others of the $[2.2.2]Cs^+$ complex,[18] which may have more thoroughly explored conformation space, predict that at minimum energy the metal lies *inside* the binding cavity, near the center of mass of the ligand.

In summary, both the 2:1 complexation results and molecular models suggest that in the gas phase the [2.1.1] cavity is approximately large enough to accommodate Na^+, that [2.2.1] can contain K^+, and that the [2.2.2] cavity is large enough to

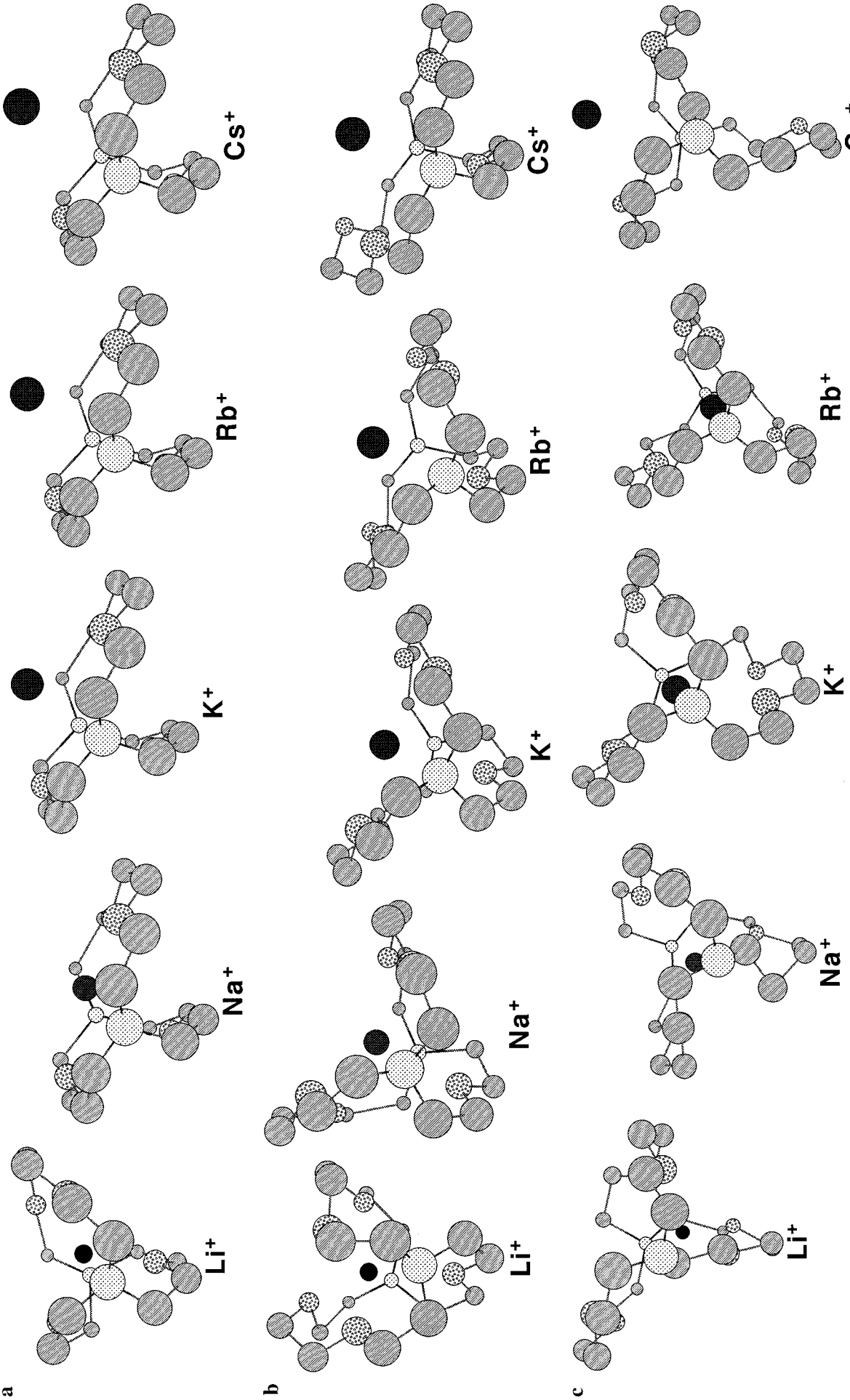

Figure 2. Minimum-energy structures of alkali metal cryptates generated using the AMBER molecular mechanics force field: (a) [2.1.1] cryptates; (b) [2.2.1] cryptates; and (c) [2.2.2] cryptates.

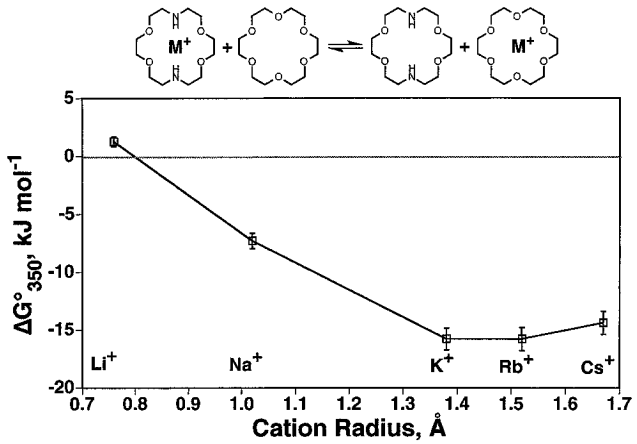

Figure 3. Gas-phase free energies of alkali cation transfer from 1,10-diaza-18-crown-6 to 18-crown-6, from equilibrium measurements at 350 K.

hold Cs^+. Further support for this interpretation is found in the thermochemical data discussed below.

Cryptate and Size-Selection Effects in the Gas Phase. In solution, it is observed that the macrobicyclic cryptands form alkali cation complexes which are more stable (by 4−5 log *K* units) than those of their monocyclic counterparts, and that the cation selectivity of cryptands is greater than that of structurally-similar crown ethers.[9] Further, solvation and ion pairing involving cryptand-complexed ions is diminished relative to either uncomplexed cations or cations bound by monocyclic ligands, since the cation is isolated by the 3-dimensional ligand from the external environment. These effects, known as *cryptate effects*, are in general larger than the macrocyclic effects which are seen when acyclic and monocyclic ligands are compared. Cryptate effects in solution have been shown to be largely enthalpic in origin.[3]

As an extension of our earlier work which found pronounced macrocyclic effects in gas-phase ion−molecule reactions,[44,45] two types of experiment were designed to probe cryptate effects in the gas phase. In the first, macromonocyclic crown ethers and macrobicyclic cryptands, each with the *same number of heteroatom donor groups*, were allowed to compete for alkali metal cations. The second type of experiment involved competition between crown ethers and cryptands having *portals of approximately the same size as the crown*. Both types of experiment showed cryptate effects, which to our knowledge are the first to be noted in the gas phase.

All of these experiments depend to some extent on the assumption that the behavior of oxygen and nitrogen donor atoms toward alkali metal cations is similar. To test this assumption, equilibrium constants were measured for transfer of alkali metal cations from 1,10-diaza-18-crown-6 (DA18C6) to 18C6. For all the alkali metal cations except Li^+, the nitrogen-for-oxygen substitution led to *decreased* complex stability in the gas phase (Figure 3). Therefore, we might expect the nitrogen atoms in cryptands to be less effective donors toward alkali metal cations than crown ether oxygens. The degree of binding preference for 18C6 over DA18C6 correlates roughly with cation size, becoming larger as cation size increases. Similar effects have been noted previously in studies carried out in methanol solution, which found complexation by DA18C6 to be far weaker than that involving 18C6.[57]

These results can be rationalized by noting that each of the nitrogen donors are covalently bound to hydrogen, in addition to the two carbon atoms which join them to the macrocyclic

(57) Buschmann, H. J. *Inorg. Chim. Acta* **1986**, *125*, 31−35.

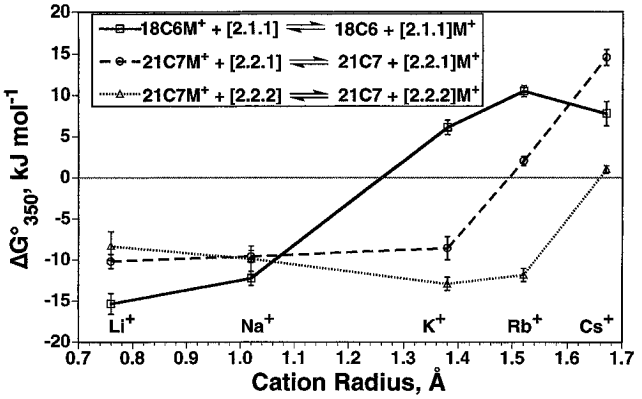

Figure 4. Gas-phase free energies of alkali cation transfer from crown ethers to cryptands, from equilibrium measurements at 350 K.

ring. The hydrogens disrupt the binding cavity of the ligand, in effect dividing the cavity into two smaller metal binding sites rather than one large binding cavity. These "mini cavities" are too small to accommodate any of the alkali metal cations except Li^+. Models indicate Li^+ is about the right size to fit into the "minicavity", which may account for the increased Li^+ affinity of the nitrogen-substituted crown. Electronic effects may also be important: geometries for the Li^+−DA18C6 complex optimized using semiempirical AM1 calculations have the nitrogen lone pairs oriented directly toward the metal.

In two sets of experiments, equilibrium constants were measured for metal transfer between crown ether and cryptand ligands with the same number of donor atoms (Figure 4). Both 18C6 and [2.1.1] have six donor groups: all six are ether oxygens in 18C6, while [2.1.1] includes four ether oxygens and 2 tertiary amine nitrogens. The cryptand has the higher affinity for Li^+ and Na^+, while 18C6 binds the larger alkali metal cations more strongly than [2.1.1]. Likewise, both 21C7 and [2.2.1] have seven donor groups: all oxygens in the case of the crown, five oxygens and two nitrogens in the case of the cryptand. [2.2.1] has higher affinity than the crown for Li^+, Na^+, and K^+. Cation transfer is nearly thermoneutral for Rb^+, with the cryptand having a Rb^+ affinity about 2 kJ mol^{-1} greater than that of the crown. Transfer of Cs^+ from the cryptand to the crown is about 14 kJ mol^{-1} exothermic.

In both sets of experiments, a remarkable change in ligand binding preference occurs as the cations become larger. This can be understood in terms of a gas-phase cryptate effect: in cases where the cations are small enough to enter the binding cavity of the cryptand, the cation affinity of the cryptand is *greater* than that of a monocyclic ligand with the same number of donor atoms. According to X-ray data,[10] the binding cavity in a cryptate complex is distinctly three-dimensional, with donor atoms well-situated for binding a spherically-symmetric guest such as an alkali metal cation. On the other hand, in crown ethers the donor atoms are constrained by the macrocyclic ring to lie in the "pseudoplane" of the ring; they cannot conform as well as the cryptand donors to the spherical symmetry of the guest, so the affinity of the cryptand for the small cations is higher. Electronic effects favoring nitrogen over oxygen donors may be important in the case of Li^+, as noted above. However, even in cases where nitrogen-for-oxygen substitution should *lower* affinity for the other alkali cations, the cryptands have *higher* affinity for the metals than do the crowns, if the metals are small enough to fit inside the cryptand cavity. This suggests proper arrangement of the donor groups, rather than electronic effects, is the dominant factor.

A reversal of binding preferences occurs when the cations become large enough that they are unable to easily enter the

binding cavity of the cryptand. In these cases, the metal most likely binds on the face of the ligand where it can maximize contacts with the most donor groups. The molecular mechanics models (Figure 2) support this idea. In the K^+, Rb^+, and Cs^+ cryptates of [2.1.1], the calculations find that in each case the metal is bound to the 15-membered face of the ligand where it is in van der Waals contact with five of the donor atoms, while the sixth donor is held some distance away by the ligand framework. The 12-membered face, with only four donor groups in proximity, is unoccupied. Likewise for [2.2.1], model calculations on the Cs^+ and Rb^+ cryptates both find the metals bound on the 18-membered face of the ligand, in contact with six of the donor atoms (the 5-donor, 15-membered faces are less-favorable binding sites). The ligand skeletal structure prevents close contact with the seventh donor. In contrast, the monocyclic structures of the crown ethers allow all of the crown oxygen donors to be in simultaneous contact with the larger cations, with the result that the cation affinities of the crowns are greater than those of the corresponding cryptands when the metals are too large to enter the cryptands' binding cavities.

The magnitude of the cryptate effect can be defined in terms of the range of variation in $\Delta G°$ as mono- and bicyclic ligands with equal numbers of donor groups are compared and the guest alkali metal ion is varied. For example, in the 18C6−[2.1.1] system the minimum in $\Delta G°$ occurs for Li^+, at about −15 kJ mol^{-1}, while the maximum occurs for Rb^+, at about +10 kJ mol^{-1}, giving 25 kJ mol^{-1} as the full magnitude of the effect in this system. Similarly, for 21C7−[2.2.1], the minimum again occurs at Li^+ (−10 kJ mol^{-1}), while the maximum is seen for transfer of Cs^+ (+15 kJ mol^{-1}), again giving 25 kJ mol^{-1} as the magnitude of the effect. As was noted above, this involves loss of one ether oxygen donor group for either [2.1.1] or [2.2.1] as the metals become too large to enter the binding cavity and come in proximity with all the donors. It would be interesting to compare the 8-donor ligands 24-crown-8 and [2.2.2] to see whether the effect becomes greater when the cryptand structure forces loss of *two* donor groups as metals become too large to enter the cryptand cavity. Unfortunately, this was not possible since the cavity of [2.2.2] apparently accommodates even the largest metal studied, Cs^+.

Further insight into the cryptate effect can be obtained by comparing crowns of a given ring size with cryptands whose largest face is the same size. In these comparisons, we would expect the greater polarizabilities of the cryptands, as well as inductive effects arising from the additional donor atom(s) of the cryptands, to lead to higher cation affinities than are found for the smaller, less polarizable crowns. The data of Table 2 bear out this prediction: [2.1.1] has higher alkali cation affinities than 15C5, and both [2.2.1] and [2.2.2] have higher affinities than 18C6.

Although neither the face size nor the total number of donors match in the case of the [2.2.2]−21C7 pair, it is interesting to note that [2.2.2] has the higher affinity for all the alkali cations except Cs^+ (Figure 4). Cs^+ is probably too large for optimal bonding to the cryptand. Accommodation of this large ion in the binding cavity may incur a substantial energetic penalty due to strain in the ligand, or perhaps the cation is simply too large to come into intimate contact with all 8 donor atoms. On the other hand, Cs^+ is a fairly good size match for the 7-donor crown, and much less strain is probably needed to accommodate the cation.

The cation size at which equilibrium shifts from favored binding of the cryptand to favored binding of the crown is in good agreement with the size arguments presented above based on kinetics and on molecular models. It is probably reasonable

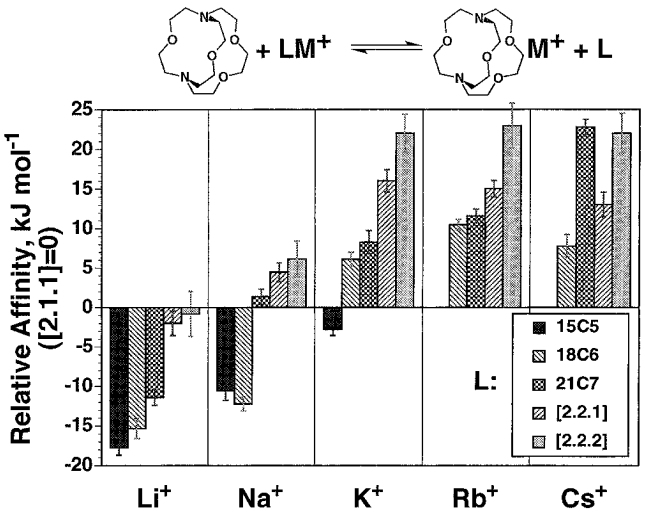

Figure 5. Alkali cation affinities of crown ethers and cryptands relative to those of [2.1.1] in the gas phase. The plotted values are means ±1 standard deviation from replicate measurements.

to estimate the cavity sizes of the ligands in the gas phase from the "crossover point" where equilibrium shifts from preferential binding of the cryptand to preferential binding of the crown as cation size increases. In the 18C6−[2.1.1] comparison, the change occurs between Na^+ and K^+, in agreement with the 2:1 complexation patterns and the AMBER models, all of which suggest Na^+ is bound inside the cavity and that K^+ is not. From Figure 4, the estimated radius of the [2.1.1] cavity in the gas phase is about 1.25 Å. Likewise, both 2:1 complexation and models indicate that [2.2.1] is large enough to encapsulate K^+, but not Rb^+, and it is between these two metals that equilibrium shifts in the 21C7−[2.2.1] system. The radius of the [2.2.1] cavity estimated from Figure 4 is about 1.50 Å. For [2.2.2], the results are less clear. The lack of observed 2:1 complexation for any of the alkali cations suggests even Cs^+ may fit inside [2.2.2], but molecular models and the 21C7−[2.2.2] thermochemistry both imply that the fit is far from optimal. From the thermochemical data of Figure 4, the [2.2.2] cavity radius in the gas phase is about 1.65 Å.

Intrinsic Alkali Cation Affinities. Gas-phase proton transfer equilibrium measurements have long been used to build proton affinity and gas-phase basicity ladders.[27−29,58] Strictly speaking, proton affinities refer to changes in enthalpy which occur upon protonation, while the corresponding free energy changes yield gas-phase basicities. Our equilibrium measurements yield free energy changes which occur on transferring alkali cation guests between host molecules, and so should properly be termed as measurements of relative basicities with respect to the various alkali metal cations. However, we find this terminology cumbersome, and so refer to the $\Delta G°$ data in terms of relative cation affinities. With the $\Delta G°$ values derived from the equilibrium constant data of Table 2, relative alkali cation affinity ladders for the various ligands in the gas phase can be established. The results for the intrinsic (i.e., independent of solvent or counterion effects) Li^+, Na^+, K^+, Rb^+, and Cs^+ affinities of the various ligands are shown in Figure 5.

Cation transfer equilibrium was observed between [2.1.1] and 15C5, 18C6, [2.2.1], and, in one case, [2.2.2], yielding direct cation affinity comparisons. Since [2.1.1] is the common ground for many of the direct measurements, we have arbitrarily chosen its alkali cation affinity as the zero point for each of our relative affinity ladders. In a number of cases, the values of Figure 5

(58) Szulejko, J. E.; McMahon, T. B. *J. Am. Chem. Soc.* **1993**, *115*, 7839−7848.

could be derived from more than one thermodynamic cycle. In these cases, results from the various pathways were averaged, and standard deviations from replicate measurements were propagated, to arrive at the values given in the figure.

What factors contribute to alkali cation affinity in the gas phase? Since the interactions between an alkali metal cation and the donor groups of the host are believed to be largely electrostatic in nature,[59−65] complexation must involve a trade-off between maximizing the host−guest electrostatic interactions and minimizing the strain induced in the structure of the host in the process of accommodating the guest. In addition, the number of donor groups, and the polarizability of the ligand, should also play important roles. We expect the intrinsic affinity to be higher for the smaller cations, since they can in general come into closer contact with the donor atoms and are stronger polarizers than the larger, more diffuse cations. High-level *ab initio* calculations for 18C6−alkali cation complexes[65] also predict this trend.

Cryptate effects can easily be rationalized in these terms, since in properly-sized cryptands the donors are prearranged in a favorable geometry and little additional strain accompanies complexation. Conversely, if the size match between host and guest is poor, the relative rigidity of the cryptand structure prevents it from maximizing the cation−donor interactions and binding is relatively weak.

The high selectivity of gas-phase [2.1.1] for Li^+ is clearly evident, since this ligand has higher Li^+ affinity than any of the simple crowns and roughly the same as the bigger cryptands [2.2.1] and [2.2.2]. This parallels the Li^+ selectivity of [2.1.1] in water, 95:5 methanol−water, and pure methanol solutions.[9] The intrinsically high Li^+ affinity of [2.1.1] is not particularly surprising in light of the concept of ligand prearrangement: Li^+ is a good match for the [2.1.1] cavity, according to molecular models, X-ray data,[54] and 2:1 complexation kinetics. Further, in [2.1.1] the donor groups are arranged in three dimensions, so that cryptate effects favor this ligand over similar-sized monocyclic ligands.

Generally, affinities for a given cation increase in the order 15C5 < 18C6 < 21C7 < [2.2.1] < [2.2.2], as might be expected based on cryptate effects and the polarizabilities and number of donors for the various ligands. There are two exceptions to this trend. The Na^+ affinity of 15C5, measured relative to that of [2.1.1], is slightly greater than that of 18C6, although direct comparison of the two crowns[44] shows the larger ligand has the greater Na^+ affinity. This disagreement might easily be explained through errors in the relative pressures of the ligands being compared. In addition, it is possible that the Na^+ affinity of 15C5 really is anomalistically high; X-ray data suggest Na^+ is approximately the right size to fit in the 15C5 cavity. The other clear exception, which is less likely to be explained by errors in pressure measurement, also involves possible size match between a metal ion and a crown cavity. Among the Cs^+ affinities, the value for 21C7 is much greater than that for [2.2.1] and about the same as that for [2.2.2]. As noted above, this is probably a prearrangement effect, since Cs^+ is too large

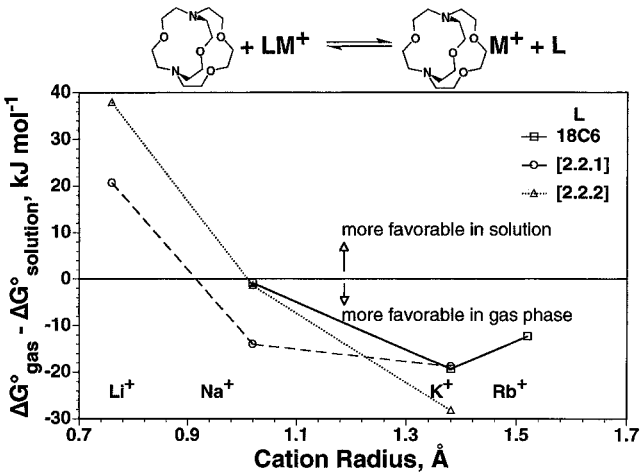

Figure 6. Differences between free energies of alkali cation transfer to [2.1.1] in the gas phase and in solution (95:5 methanol−water, for transfers from [2.2.1] or [2.2.2]; absolute methanol, for transfers from 18C6). Solution data compiled from ref 8.

to enter the [2.2.1] cavity and interact with all seven donors, and is too large to fit optimally in [2.2.2], but is about the right size to interact well with all the donors of 21C7.

It is tempting to infer cation affinity trends as a function of cation size from Figure 5, but we caution that such analyses cannot be made since there is no anchor point between the various cation affinity scales; all are simply *relative* to the cation affinity of [2.1.1]. We are currently working on *absolute* cation affinity measurements to provide anchor points which would allow the varius scales to be directly compared.[66]

Comparison of Solution and Gas-Phase Data. Solution log *K* data,[9] obtained using potentiometric methods, can be used to derive equilibrium constants and $\Delta G°$ values for cation transfer between two ligands in solution. This makes direct comparison of the solution and gas-phase results possible. Log *K* for reaction 1 in 95:5 methanol−water (L = [2.2.1] and

$$[2.1.1]_{(solution)} + LM^+_{(solution)} \rightleftharpoons [2.1.1]M^+_{(solution)} + L_{(solution)} \quad (1)$$

[2.2.2]) and in methanol (L = 18C6) was determined from the difference between log *K* values for complex formation for each of the two ligands,[7,8] and $\Delta G°$ was calculated for a temperature of 350 K. While the free energy *trends* seen in solution are approximately the same as the intrinsic trends seen in the gas phase (a monotonic increase in $\Delta G°$ from Li^+ through K^+ for reaction 1 involving all three ligands examined, for example), the *magnitude* of the trend is greatly amplified by solvation. Thus, the solvation properties of the various complexes, rather than intrinsic metal selectivities (as measured in the gas phase, in the absence of solvation), are responsible for most of the free energy change in reaction 1. This is not particularly surprising, given that stability constants for metal−ligand complexes such as these have long been known to depend strongly on the nature of the solvent. However, comparison with the gas-phase results allows the solvation effects to be quantified for the first time.

The differences between the gas-phase and solution results are plotted together in Figure 6 as a function of guest cation radius. The differences are a direct reflection of solvation effects. Positive differences mean that the transfer of metal from L to [2.1.1] is less favorable in the gas phase than in solution,

(59) Staley, R. H.; Beauchamp, J. L. *J. Am. Chem. Soc.* **1975**, *97*, 5920−5921.
(60) Woodin, R. L.; Houle, F. A.; Goddard, W. A., III *Chem. Phys.* **1976**, *14*, 461.
(61) Clementi, E.; Popkie, H. *J. Chem. Phys.* **1972**, *57*, 1077.
(62) Kistenmacher, H.; Popkie, H.; Clementi, E. *J. Chem. Phys.* **1973**, *59*, 5842.
(63) Kistenmacher, H.; Popkie, H.; Clementi, E. *J. Chem. Phys.* **1974**, *61*, 799.
(64) Rode, B. M.; Breuss, M.; Schuster, P. *Chem. Phys. Lett.* **1975**, *34*, 7.
(65) Glendening, E. D.; Feller, D.; Thompson, M. A. *J. Am. Chem. Soc.* **1994**, *116*, 10657−10669.
(66) Pope, M.; Dearden, D. V. In *43rd ASMS Conference on Mass Spectrometry and Allied Topics*; ASMS: Atlanta, GA, 1995; p 53.

while negative differences indicate the transfer is more favorable in the gas phase than under solvated conditions.

For all three ligands, L, the trends in the gas−solution differences are similar: Li^+ transfer is much more favorable in solution than in the gas phase, while transfers of the other metal ions in general become less favorable in solution than in the gas phase as the ionic radius increases. These data can be understood by considering how well the various ligands meet the inner-sphere solvation requirements of the ions, and the resulting effects on solvation entropy as the metals are transferred. As noted above, [2.1.1] is Li^+ selective. This ligand satisfies the solvation requirements of Li^+ better than any of the other host molecules examined, so that in the transfer reaction there is a net release of solvent as the metal moves from the poorer to better ligand. Transfer is therefore more favorable than in the gas phase, where there is no entropic benefit from solvent release. Because it is too small, [2.1.1] is a poorer ligand toward the larger alkali cations than any of the other hosts examined. As a result, when the metal is transferred to [2.1.1] there is a net *increase* in the number of strongly associated solvent molecules, and the transfer is *disfavored* relative to the gas phase, where there is no entropic penalty.

Details of the trends in Figure 6 are also consistent with this explanation. For example, both 18C6 and [2.2.2] are K^+ selective, suggesting that these ligands meet the solvation requirements of K^+ particularly well. Thus, transfer of the metal from these very stable complexes to [2.1.1] results in a net organization of bulk solvent molecules and the transfer is much less favorable in solution than in the gas phase. This interpretation also predicts that as the metals become large enough that neither ligand does a good job of meeting the metal solvation requirements, the gas−solution differences should become smaller. This is indeed observed in the case of L = 18C6, where the magnitude of the gas−solution difference is smaller for Rb^+ than for K^+. Similarly, we would predict a decrease in the gas−solution difference for L = [2.2.1] with increasing metal size, but the decrease should occur for larger metals for this larger ligand than in the L = 18C6 case. While this decrease is not observed, the shape of the curve in Figure 6 suggests the decrease will occur with larger metals. Likewise, the [2.2.2] complexes, involving the largest ligand, should show this effect the least, as observed.

Conclusions

The gas-phase chemistry of cryptand−alkali cation interactions can be explained largely on the basis of the size relationships between the hosts and guests. Both the patterns for 1:1 vs 2:1 ligand−metal complexation and the thermochemistry of alkali cation transfer between crown ethers and cryptands give consistent results for the sizes of the cryptand binding cavities in the gas phase, which are in most cases consistent with the results of molecular mechanics calculations. The gas-phase cavity sizes are, not surprisingly, similar to those observed in condensed media, although there is some evidence that the tendency of cryptands to form "inclusive" complexes of the metals is greater in the gas phase than in solution, where the ligands must compete with solvent and counterion species for the coordination sites around the cations.

The remarkable cation binding properties of cryptands, long known in condensed media, extend into the gas phase. The cryptands are powerful alkali cation complexing agents, particularly in cases where they are large enough for the cations to enter their binding cavities. The binding of alkali metal cations by cryptands shows very strong size dependence, providing a second example of ionic size recognition in the gas phase to complement that of the crown ethers. Large cryptate effects are observed, showing that these are intrinsic to the host−guest system, and independent of solvation. These effects have large influences on the energetics of cation transfer between gas-phase ligands, and likely should be considered as the chemistry of large, cation-attached ions, generated using electrospray or matrix-assisted laser desorption ionization, is explored.

While relative cation affinities can be measured with some confidence, much work remains to be done in establishing the absolute cation affinities of cryptands and other ligands. Estimates which yield reasonable overall trends can be made using molecular mechanics calculations, but these should be regarded as tentative. Definitive answers about the reliability of the theoretical predictions await more rigorous tests, involving experimental measurement of the absolute cation affinities.

Acknowledgment. We are grateful for the support of the Robert A. Welch Foundation (grant Y-1214), the donors of the Petroleum Research Fund, administered by the American Chemical Society (26836-AC6,4), and the National Science Foundation (CHE-9496141 and CHE-9496150).

JA953460E